ACTA METALLURGICA SLOVACA
2021, VOL. 27, NO. 4, 207-209

RESEARCH PAPER

AUSTENITE – FERRITE TRANSFORMATION TEMPERATURES OF C-MN-AL HSLA STEEL

Peter Prislupčák[1,2] *, Tibor Kvačkaj[2], Jana Bidulská[2], Pavol Záhumenský[1], Viera Homolová[3], Peter Zimovčák[1]

[1] U. S. Steel Košice, s.r.o., Research and Development USSE, Košice, Slovakia
[2] Technical University of Košice, Faculty of Materials, Metallurgy and Recycling, Košice, Slovakia
[3] Slovak Academy of Science, Institute of Materials Research, Košice, Slovakia

*Corresponding author: peterprislupcak@sk.uss.com; +421 917097744; U. S. Steel Košice, s.r.o., Research and Development USSE, Vstupný areál U. S. Steel, 044 54 Košice, Slovakia

Received: 22.11.2021
Accepted: 01.12.2021

ABSTRACT

The article is aimed to investigate a shift of transformation temperatures of C-Mn-Al HSLA steel with different cooling rates. The transformation temperatures from austenite to ferrite have been determined by dilatometry using thermal-mechanical simulator Gleeble 1500D. To define the start and finishing temperatures of the austenite-ferrite transformation intersectional method was used. Effect of cooling rate on transformation temperature has been evaluated for 0.17, 1, 5, 10, 15, 20, 25°C.s^{-1}. There was found out that rising the cooling rate results in moving transformation temperature range to lower temperatures. The transformation temperatures have been also compared with temperatures calculated using equations of several authors. Some of them have considered cooling rates only. Cooling rates have effect on final microstructure. The effect has been evaluated by measuring hardness (HV10) relating the cooling rates from 0.17 to 25°C.s^{-1}. Increasing cooling rates resulted in increase of hardness. Moreover, Thermo-Calc software was used to determine the Ae3 and Ae1 equilibrium temperatures. Equilibrium transformation temperatures Ae3-Ae1 were higher than experimentally measured by dilatometric method using Gleeble 1500D.

Keywords: HSLA steel, transformation temperatures, dilatometry

INTRODUCTION

In recent years weight savings design has taken on high importance in the automotive industry. The trend towards fuel economy and exhaust emission decrease has brought forth the requirement to construct lighter weight auto bodies [1]. It is commonly reported that a 10% reduction in vehicle mass transforms into a 6-8% reduction in fuel consumption [2].
Advanced high-strength steels (AHSS) have been developed within the last decades to meet the increasing requirements for weight reduction and improved crashworthiness properties in the automotive industry [3]. Dual-phase (DP) and low-carbon transformation-induced-plasticity (TRIP) steels are generally considered as the first-generation AHSS. The combination of the ferritic matrix and second phases offers the AHSS first-generation high strength with appropriate formability. The development of high-Mn steels with various deformation modes like TRIP, twinning-induced plasticity (TWIP) and microband-induced plasticity (MBIP) are considered as the second-generation AHSS. Quenching and partitioning (Q&P) steel, TRIP-aided bainitic ferrite steel and medium-Mn steel are well known as the AHSS of third-generation. These steels are based on the high Mn content in combination with nanostructures as well as local partitioning phenomenon [4-8].
Microalloying is an effective way in managing the processing of advanced high strength steels by their influence on recrystallization and transformation and in controlling the properties by microstructural refinement and precipitation hardening [9, 10]. Monitoring of phase transformations and the knowledge of continuous cooling transformation (CCT) diagrams are very beneficial for proper design of bainite–austenite microstructures with an optimal morphology. Decomposition of retained austenite on heating or cooling from the austenite region is common monitored by dilatometry, differential thermal analysis (DTA) or differential scanning calorimetry (DSC) [11-18].
This work is focused on finding relation of different cooling rates on austenite – ferrite transformation temperatures shifting of the C-Mn-Al HSLA steel.

MATERIAL AND METHODS

Experimental work has been performed using material concept of C-Mn-Al HSLA steel. Chemical composition of the steel is given in **Table 1**.

Table 1 Chemical composition of the C-Mn-Al HSLA steel

Component	C	Mn	Si	P	Al	Cr+Mo	Nb+Ti
Wt. (%)	max. 0.18	max. 2.1	max. 0.14	max. 0.04	max. 0.7	max. 1.0	max. 0.15

The thermal deformation simulator of physical processes Gleeble 1500D in temperature ranges of austenite to ferrite transformation for above mentioned steel was used. Standard size tensile specimens with dimensions of ∅10×110mm taken from transfer bar (i.e., semi-products during hot rolling between roughing and finishing mill) were used in the experiment. The specimens were

heated with heating rate of 25°C.s^{-1} to 1200°C. The austenitization temperature of 1200°C with holding time of 30s was applied before cooling to room temperature by cooling rates of 0.17, 1, 5, 10, 15, 20 and 25°C.s^{-1}, as shown in **Fig. 1**. To define the start and finishing temperatures of the austenite-ferrite transformation an intersectional method was used. Principle is shown in **Fig. 2**.

Moreover, hardness test has been used to differentiate between microstructures resulting from different cooling rates. Chemical composition of the C-Mn-Al HSLA steel has been determined using LECO analyzer by Optical Emission Spectral Analysis. The thermodynamic calculations were performed using Thermo-Calc software with commercial thermodynamic database TCFE6. Phase equilibria were calculated for the temperature range 400 - 1600°C.

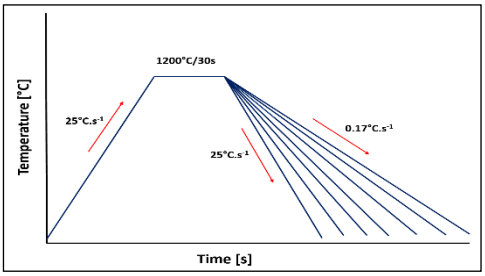

Fig. 1 Heating and cooling cycle determination of transformation temperature range

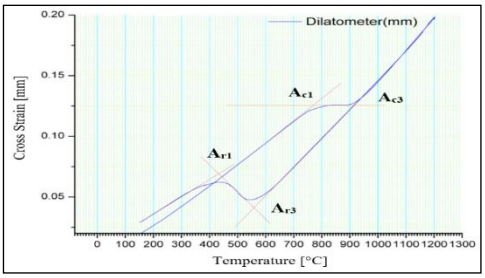

Fig. 2 Principle of transformation temperature range definition

RESULTS AND DISCUSSION

The temperature ranges [Ar_3- Ar_1] of γ→α transformation during cooling stated by dilatometry for the seven different cooling rates (0.17, 1, 5, 10, 15, 20 and 25°C.s^{-1}) via the intersectional method are listed in Fig. 3 and Table 2. For the comparison equilibrium transformation temperatures [Ae_3-Ae_1] calculated by Thermo-Calc software as well as γ→α transformation temperatures calculated by regression equations of several authors are also listed in the **Table 2**.

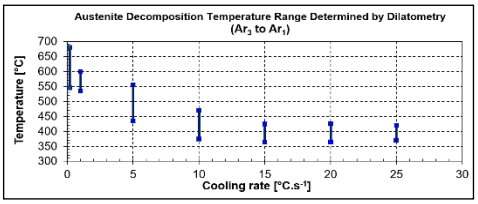

Fig. 1 Shifting the transformation temperature ranges with different cooling rates determined by dilatometry

Selected regression equations of several authors used to calculate Ar_3- Ar_1 temperature range are shown below.

Ar_3= *914 - 6.85v* - 650C - 134Mn + 179·Si* *(a)* [19]
Ar_1= *814 - 9.08v* - 532C - 121Mn + 165·Si* *(b)* [19]
Ar_3 = 903 - 328*C* – *102Mn*+ 116*Nb* – 0.909*v** *(c)* [20]
Ar_3 = 902 − 527*C* − 62*Mn* + 60*Si* *(d)* [21]
Ar_3 = 879.4 – 516.1C – 65.7Mn +38.0Si + 274.7P (e) [22]
Ar_1 = 706.4 – 350.4C – 118.2Mn (f) [22]
Ar_3 = 910 – 310C – 8Mn - 20Cu – 15Cr – 55Ni – 80Mo + 0.35(h*-8) (g) [23]
Ar_3 = 910 – 273C – 74Mn – 56Ni – 16Cr – 9Mo – 5Cu (h) [24]
Ar_3 = 910 – 230C – 21Mn – 15Ni + 32Mo + 45Si +13W + 104V (i) [25]

Where:
* *v* - cooling rate [°C.s^{-1}]
* h - sample thickness [mm]
Components [Wt. (%)]

Hardness test has been used for the same seven different cooling rates using HV10. The results are given in **Table 3**.

Table 2 Transformation temperatures of the C-Mn-Al HSLA steel at different cooling rates

Cooling rate	Determined by dilatometry	Calculated by Thermo-Calc	Calculated by regression equations						
			a	**b, c**	**d**	**e, f**	**g**	**h**	**i**
[°C.s^{-1}]	**(Ar_3 – Ar_1) [°C]**	**(Ae_3 – Ae_1) [°C]**	**(Ar_3) [°C]**	**(Ar_3 – Ar_1) [°C]**	**(Ar_3) [°C]**	**(Ar_3 – Ar_1) [°C]**	**(Ar_3) [°C]**	**(Ar_3) [°C]**	**(Ar_3) [°C]**
0	-	894-688	648	563 - 506	696	674 - 410	837	711	828
0.17	680 - 545	-	648	562 - 505	-	-	-	-	-
1	600 - 538	-	647	557 - 497	-	-	-	-	-
5	555 - 435	-	643	529 - 461	-	-	-	-	-
10	470 - 375	-	639	495 - 416	-	-	-	-	-
15	445 - 365	-	634	462 - 370	-	-	-	-	-
20	425 - 365	-	630	426 - 325	-	-	-	-	-
25	420 - 370	-	625	392 - 280	-	-	-	-	-

Table 3 Hardness of the C-Mn-Al HSLA, HV10

Cooling rate [°C.s^{-1}]	0.17	1	5	10	15	20	25
HV10	209	214	239	316	403	403	402

Transformation temperatures change with the cooling rate therefore they were stated for seven different cooling rates (0.17, 1, 5, 10, 15, 20 and 25°C.s^{-1}). The results of γ→α transformation determined by dilatometry using Gleeble 1500D are given in Fig. 3 and Table 2. There was found out that cooling rates up to 15°C.s^{-1} have significant effect on transformation temperatures. Raising the cooling rate results in moving transformation temperature range to lower temperatures as you can see in Fig. 3.

While at the lowest achieved cooling rate of 0.17°C.s^{-1}, the temperature range of Ar_3-Ar_1 was 680 to 545°C, from the cooling rate of 15°C.s^{-1} and more, the Ar_3-Ar_1 temperature range was 445 to 365°C. Many authors [19-25] defined several regression equations for starting γ→α transformation temperatures. Some of them have considered cooling rates only [19, 20]. Generally, chemical composition, cooling rate, and strain have effect on transformation temperature. The transformation temperatures stated experimentally have been compared with those calculated using equations of several authors. Comparing our measured results with those calculated equations a, b, c [19, 20] it can be stated that notable differences have been found because of different chemistry. The smallest differences between measured and calculated results regarding Ar_3 temperature can be seen for the lowest cooling rate 0.17°C.s^{-1} for the equation (c) [20] and for cooling rate 20°C.s^{-1} for the equations (a, b) [19]. Other regression equations (d-i) [21-25] don´t consider cooling rate. The most similar chemistry is given in equation (d, f) [21, 22]. Although, the major alloying elements of the experimental material are very similar to those in equations (d, f) [21, 22] the transformation temperatures are notable different. This can result from absence of cooling rate effect in the above mentioned equations. Transformation temperatures calculated by Thermo-Calc software are higher than experimentally measured by dilatometric method using Gleeble 1500D resulting from high cooling rates comparing to equilibrium conditions used in Thermo-Calc software. Cooling rates have effect on final microstructure. The effect has been evaluated by measuring hardness (HV10). Increasing cooling rates result in increase of hardness as you can see in **Table 3**.

The novelty of the present work includes the identification of γ→α transformation temperatures of the C-Mn-Al HSLA Steel.

CONCLUSION

Based on the results achieved in this work focused on γ→α transformation temperatures of the experimental steel, the following conclusions can be stated:

- Transformation temperatures have been evaluated for 7 different cooling rates (0.17, 1, 5, 10, 15, 20 and 25°C.s^{-1}) determined by dilatometry using Gleeble 1500D. While at the lowest achieved cooling rate of 0.17°C.s^{-1}, the temperature range of Ar_3-Ar_1 was 680 to 545°C, from the cooling rate of 15°C.s^{-1} and more, the Ar_3-Ar_1 temperature range was 445 to 365°C.
- Equilibrium transformation temperatures Ae_3-Ae_1 calculated by ThermoCalc software were higher than experimentally measured by dilatometric method using Gleeble 1500D. The Ae_3-Ae_1 temperature range was 894 to 688°C.
- The transformation temperatures stated experimentally have been compared with regression equations of several authors. The smallest differences between measured and calculated results regarding Ar_3 temperature can be seen for the lowest cooling rate 0.17°C.s^{-1} for the equation (c) and for cooling rate 20°C.s^{-1} for the equations (a, b).
- Knowing the austenite to ferrite transformation temperatures allows the process parameters to be better controlled during hot rolling.

REFERENCES

1. H. Hofmann, D. Mattissen, T.W. Schaumann: Steel Research International, 80(1), 2009, 22-28. https://doi.org/10.2374/SRI08SP113.
2. Ch. Lesch, N. Kwiaton, F.B. Klose: Steel Research International, 88(10), 2017, 1700210. https://doi.org/10.1002/srin.201700210.
3. O. Bouaziz, H. Zurob, M. Huang: Steel Research International, 84(10), 2013, 937-947. https://doi.org/10.1002/srin.201200288.
4. W. Bleck, X. Guo, Y. Ma: Steel Research International, 88(10), 2017, 1700218. https://doi.org/10.1002/srin.201700218.
5. L. Liu, B. He, M. Huang: Advanced Engineering Materials, 20(6), 2018, 1701083. https://doi.org/10.1002/adem.201701083.
6. O. Bouaziz, S. Allain, C.P. Scott, P. Cugy, D. Barbier: Current Opinion in Solid State and Material Science, 15(4), 2011, 141–168. https://doi.org/10.1016/j.cossms.2011.04.002.
7. T. Kvačkaj: Structures and properties formation by plastic deformations. In.: *24th International Conference on Metallurgy and Materials - METAL 2015*, Tanger: Brno, Czech Republic, 2015, p. 28-34.
8. T. Kvačkaj, J. Bidulská: Materials Science Forum, 783-786, 2014, 842-847. https://doi.org/10.4028/www.scientific.net/MSF.783-786.842.
9. W. Bleck, K. Phiu-On: Material Science Forum, 500-501, 2005, 97-114. https://doi.org/10.4028/www.scientific.net/MSF.500-501.97.
10. T. Kvačkaj, J. Bidulská, R. Bidulský: Materials, 14(8), 2021, 1988. https://doi.org/10.3390/ma14081988.
11. J. Sas, T. Kvačkaj, O. Milkovič, M. Zemko: Materials, 9(12), 2016, 970-978. https://doi.org/10.3390/ma9120971.
12. T. Kvačkaj, J. Bacsó, J. Bidulská, M. Lupták, I. Pokorný, M. Kvačkaj, M. Vlado: Acta Metallurgica Slovaca, 16(4), 2010, 268-276.
13. D. Bublíková, H. Jirková, K. Rubešová, M. Peković, J. Volkmannová, M. Graf: Acta Metallurgica Slovaca, 25(2), 2019, 93-100. https://doi.org/10.12776/ams.v25i2.1266.
14. L. Némethová, T. Kvačkaj, R. Mišičko, I. Pokorný, I. Kovárová: Acta Metallurgica Slovaca, 15(3), 2009, 173-179.
15. A. Gazda: Journal of Thermal Analysis and Calorimetry, 102, 2010, 923-930. https://doi.org/10.1007/s10973-010-0804-y.
16. L. Zhao, K. Top, V. Rolin, J. Sietsma, A. Mertens, P. Jacques, S.V. Zwaag: Journal of Materials Science, 37, 2002, 1585-1591. https://doi.org/10.1023/A:1014941424093.
17. M. Gojic, M. Suceska, M. Rajic: Journal of Thermal Analysis and Calorimetry, 75, 2004, 947-956. https://doi.org/10.1023/B:JTAN.0000027188.58396.03.
18. A. Grajcar, W. Zalecki, P. Skrzypczyk, A. Kilarski, A. Kowalski, S. Kolodziej: Journal of Thermal Analysis and Calorimetry, 118, 2014, 739-748. https://doi.org/10.1007/s10973-014-4054-2.
19. J.G. Blás: Influência da Composição Química e da Velocidade de Resfriamento sobre o Ponto Ar3 em Amos de Baixo C Microligados ao Nb. In: *Congresso Anual da Associação Brasileira de Metais*, ABM: São Paulo, Brasil, 1989, Vol. 1, p. 11-29.
20. P. Záhumenský, I. Kohútek, J. Semeňák: IOP Conference Series: Materials Science and Engineering, 283, 2017, 012024. http://dx.doi.org/10.1088/1757-899X/283/1/012024.
21. P. Choquet: Mathematical Model for Predictions of Austenite and Ferrite Microstructures in Hot Rolling Processes. In.: IRSID Report, St. Germain-en-Laye, 1985, p. 7.
22. A.A. Gorni: Steel Forming and Heat Treatment Handbook. Edition: 13 December 2019. On-Line. http://www.gorni.eng.br/e/Gorni_SFHTHandbook.pdf.
23. C. Ouchi: Transactions of the ISIJ, 22, 1982, 214-222. https://doi.org/10.2355/isijinternational1966.22.214.
24. C. Shiga, et al.: Kawasaki Steel Technical Report, (4), 1981, 97-109. https://www.jfe-steel.co.jp/archives/en/ksc_giho/no.04/e4-097-109.pdf.
25. F.B. Pickering: Steels: Metallurgical Principles. In: *Encyclopedia of Materials Science and Engineering*, Vol. 6, MIT Press: Cambridge, 1986.